Thermal conductivity of rare-earth element dodecaborides

1995 J. Phys.: Condens. Matter 7 8927

(http://iopscience.iop.org/0953-8984/7/47/013)

J. Phys.: Condens. Matter 7 (1995) 8927–8937. Printed in the UK

Thermal conductivity of rare-earth element dodecaborides

H Misiorek†, J Mucha†, A Jeżowski†, Y Paderno‡ and N Shitsevalova‡

† Institute of Low Temperature and Structure Research, Polish Academy of Sciences, PO Box 937, 50–950 Wrocław, Poland

‡ Institute for Problems of Materials Science, Academy of Sciences of Ukraine. 3 Kzhyzhanovski Street, Kiev 252680, Ukraine

Received 24 October 1994, in final form 25 August 1995

Abstract. Measurements of the thermal conductivities of rare-earth element dodecaborides REB_{12} (RE = Tb, Dy, Ho, Er, Tm or Lu) were conducted in the temperature range 4.2–300 K. The temperature dependences of the electronic and phonon thermal conductivities in the paramagnetic-to-antiferromagnetic transition range were determined. For TmB_{12} and HoB_{12} the Lorenz function exhibits a distinct variation relative to L_0 (L_0 is the theoretical value of the Lorenz function) in the temperature range 50–90 K. By comparing the electronic and phonon thermal conductivities of the magnetic compounds (with Tb, Dy, Ho, Er and Tm) with the same quantities for nonmagnetic LuB_{12}, the influence of the interaction of electrons and phonons with 4f electrons on the heat transport was calculated. By the same token, we elucidated the influence of crystal electric field on the thermal conductivity of the REB_{12} compounds.

1. Introduction

The dodecaborides that we investigated were formed with the rare earth (RE) elements Y and Gd–Lu. These compounds crystallize in a FCC structure of the UB_{12} type (O_h^5 ($Fm3m$)) originating from the NaCl structure, in which Na ions are replaced by RE atoms and Cl ions by the B_{12} cubooctrahedra. However, this structure may be also considered as composed of two sublattices: boron and metal. The existence of these sublattices, being relatively shifted to one another by one half of the unit-cell parameter, determines in many cases the individual physical properties of these compounds. High values of melting temperature and microhardness, vague variation in lattice parameters with increasing RE atomic number, and weak temperature dependence of the thermal expansion coefficient at medium and high temperatures are all connected with a rigid boron sublattice which is formed by the B_{12} structure elements. The links between B_{12} cubooctahedra in the sublattice and within B_{12} complexes are determined by strongly covalent B–B bonds [1–3].

The metallic character of these compounds finds theoretical support in the calculations of band structures [4].

All the samples analysed exhibit a constant valency, +3, whereas, for YbB_{12}, an effect of valence fluctuation was also found [5, 6].

The lower values of thermal conductivity of our samples compared to those of the constituting RE elements themselves are the result of a stronger influence of lattice vibrations on the electronic heat transport in REB_{12} [7]. The diamagnetism of ScB_{12}, YB_{12} and LuB_{12} as well as antiferromagnetic ordering of TbB_{12}, DyB_{12}, HoB_{12}, ErB_{12} and TmB_{12} result from the 4f-shell filling, i.e. from the ion nature of the compounds [8, 9].

0953-8984/95/478927+11$19.50

Detailed studies of REB_{12} transport and magnetic properties have hitherto been carried out on sintered or remelted polycrystalline samples and, except for YbB_{12}, at temperatures above that of liquid nitrogen [8–11], whereas the main peculiarities of the behaviour of kinetic coefficients take place at liquid-helium temperature. In general, the magnetic properties data from the low-temperature range concerned the magnetic ordering temperatures [6].

The discrepancies between the data from various research groups are evidently caused by the different qualities of the samples studied.

To our knowledge, only one publication has been devoted to the study of the thermal conductivity of dodecaborides over the temperature range 300–1000 K [11].

Taking into account the foregoing, this paper is aimed at carrying out a study of the thermal conductivities of the REB_{12} samples (RE = Tb, Dy, Ho, Er, Tm or Lu) over a wide temperature range and making, on this basis, an analysis of the electronic and phonon contributions to this effect. The electrical resistivity data obtained on the same sample are used in the thermal conductivity analysis.

2. Experimental details

The process of sample preparation comprises the following stages: the synthesis of dodecaborides by borothermic reduction of Tb, Dy, Ho, Er, Tm and Lu oxides *in vacuo* at 1800–2000 K, compacting the thus received powders by slip casting into rods, *in-vacuo* sintering at 2000 K and the process of inductive zone melting.

We elaborated the technology of sample preparation by inductive zone melting applicable to dodecaborides. The composition of the melted samples obtained exhibits a distinct shift in the component ratio towards an increasing metal content, up to $RE_{1.07}B_{12}$, regardless of the metal nature of the compounds. The excess boron which emerges during melting evaporates or goes into the melting zone. Hence, despite the peritectic character of REB_{12} melting [1], we succeeded in obtaining single-phase samples using a selected combination of the main technological parameters: crystallization rate, inter-gas pressure, the starting composition of substrates, etc. The almost constant nature of the lattice parameters for dodecaboride samples, regardless of composition (REB_{12}–$RE_{1.07}B_{12}$) [12], indicates the important role of rigid covalent B–B bonds in the lattice formation.

We obtained DyB_{12} in a polycrystalline form, and HoB_{12}, TmB_{12}, ErB_{12} and LuB_{12} in single-crystal forms. The use of oriented seeds and high-purity source materials and the removal of some impurities by zone melting allowed us to produce high-purity Ho, Er, Tm and Lu dodecaboride single crystals. Their main orientations were [100], [110] and [111]; they consisted of large blocks with misorientation less than 0.5°. The total content of impurities did not exceed 1×10^{-2}%.

It was not possible to prepare TbB_{12} single-phase melted samples, despite the use of a pressure up to 2.2 MPa and a crystallization rate up to 10 mm min^{-1}. This compound tends to decompose during melting, which results in a mixture of TbB_4, TbB_6 and TbB_{12} phases. Evidently, the instability of TbB_{12} is related to its position at the edge of existence of a given structure type in the phase diagram. Therefore, TbB_{12} samples were used for further investigation in the sintered form, their composition being close to nominal stoichiometry.

The samples were rectangular parallelepipeds about 2 mm × 2 mm × 8 mm in size. The density of the samples investigated was calculated from the lattice parameters (table 1).

All the samples have also been subjected to an x-ray diffraction investigation, confirming the undistorted cubic structure of the compounds.

The thermal conductivity measurements were performed using the stationary heat flux

Table 1. Density of dodecaboride samples calculated from lattice parameters.

Sample	Density (g cm^{-3})
LuB_{12}	4.727
TbB_{12}	4.536
DyB_{12}	4.516
HoB_{12}	4.555
ErB_{12}	4.607
TmB_{12}	4.652

method in the temperature range 4.2–300 K. The experimental set-up and the procedure has been described in detail in [13]. The sample temperature was measured with a constantan–manganin thermocouple, with liquid-nitrogen and liquid-helium temperatures as reference points. The temperature difference along the sample was 0.2 K. The time of temperature stabilization between two consecutive experimental points was 1 h above 78 K, decreasing to 15 min at temperatures of about 10 K. Particular care was taken to avoid a parasitic heat transfer between the sample and its environment. The sample was placed inside a cylindrical screen made of material displaying a thermal conductivity similar to that of the sample, along which the temperature gradient was identical with that along the sample. The mean temperatures of the sample and the screen were also identical. All current and voltage leads were thermally anchored to the screen.

The measurement error was below ±2% and the surplus error, estimated from the scatter in the measurement points, did not exceed ±0.2%.

The electrical resistivity of the same samples was recently measured [14].

3. Results and discussion

It is generally assumed that the total thermal conductivity λ is the sum of three contributions:

$$\lambda = \lambda_e + \lambda_{ph} + \lambda_m \tag{1}$$

where λ_e, λ_{ph} and λ_m are electronic, phonon and magnon thermal conductivities, respectively. Assuming that all the scattering mechanisms responsible for the thermal resistivity of a metal are additive (the Matthiessen rule), the electronic contribution to the thermal conductivity can be expressed as follows:

$$1/\lambda_e = W_e = W_{e,i} + W_{e,ph} + W_{e,m}. \tag{2}$$

The particular terms occurring in the above equation denote the thermal resistivity due to collisions of conduction electrons with lattice imperfections, phonons and magnetic moments, respectively. A similar formula can also be written for the phonon component of the thermal conductivity:

$$1/\lambda_{ph} = W_{ph} = W_{ph,i} + W_{ph,e} + W_{ph,ph} + W_{ph,m} \tag{3}$$

where the subsequent terms characterize scattering of phonons on impurities and defects, conduction electrons, lattice vibrations and magnetic moments, respectively.

Lattice vibrations can transfer an ion from an energy level to another with the absorption of a phonon. Thus, in our case, paramagnetic rare-earth ions with unfilled inner shells are the point defects which reduce the phonon thermal conductivity of the crystal lattice. The f shells are found deep in atoms, screened by the outer shells, and their splitting by the crystal

field is small (about 100 K), which is just inside the phonon energy spectrum. (Phonons can be trapped also by the levels of the d shell split by the crystal field, but interactions of the crystal field with d and f shells are significantly different.)

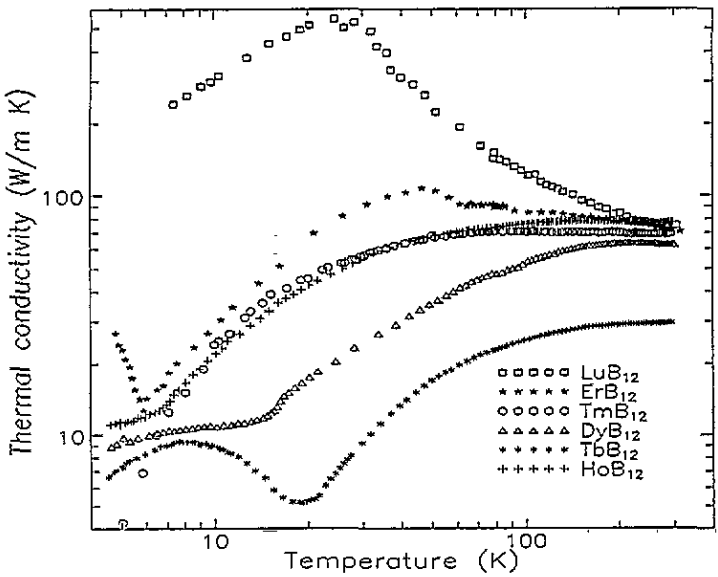

Figure 1. Temperature dependence of thermal conductivity.

Figure 1 shows the temperature dependences of the thermal conductivity λ of REB_{12}. Distinct anomalies in these $\lambda(T)$ plots are observable around the Néel temperature T_N. For DyB_{12} (T_N = 16.2 K) and HoB_{12} (T_N = 6.8 K), the derivative $d\lambda/dT$ does not change sign at the antiferromagnetic transition as occurs for ErB_{12} (T_N = 5.9 K) and TbB_{12} (T_N = 19.2 K). Nonmagnetic LuB_{12} displays a typical maximum, at about 25 K, characteristic of a pure metal or dielectric. The $\lambda(T)$ dependence of ErB_{12} shows a flat maximum at 47 K. Above 200 K, none of the thermal conductivities of compounds depends on temperature, being equal to 30 W mK^{-1} for TbB_{12} and 60–80 W mK^{-1} for the other compounds. The lower values of λ for TbB_{12} and DyB_{12} compared to the other samples are caused by the difference in quality due to the sample preparation technology (ErB_{12}, HoB_{12}, TmB_{12} and LuB_{12} are single crystals whereas DyB_{12} is polycrystalline and TbB_{12} is sintered). Photographs of these samples, obtained using scanning electron microscopy (Philips SEM-515) are presented in figure 2. A distinct qualitative difference is obvious, which corresponds to the data in figure 1. On the other hand, the x-ray diffraction investigation of these samples confirmed that their cubic structure was undistorted.

Figure 3 presents the electronic contribution λ_e to the thermal conductivity calculated from the Wiedemann–Franz (W–F) law $\lambda_e\rho/T = L_0$ ($L_0 = 2.45 \times 10^{-8}$ W Ω K^{-1} is the Lorenz constant and ρ is the electrical resistivity, the values of which for all the samples were taken from [14]). Above T_N, the temperature dependences of λ_e for our samples are similar to those of the total thermal conductivity. Below T_N, a weak dependence of λ_e on temperature is observed in contrast with the pronounced increase in the total thermal conductivity for ErB_{12}. An interesting behaviour of the electronic contribution to the thermal conductivity is observed at around T_N.

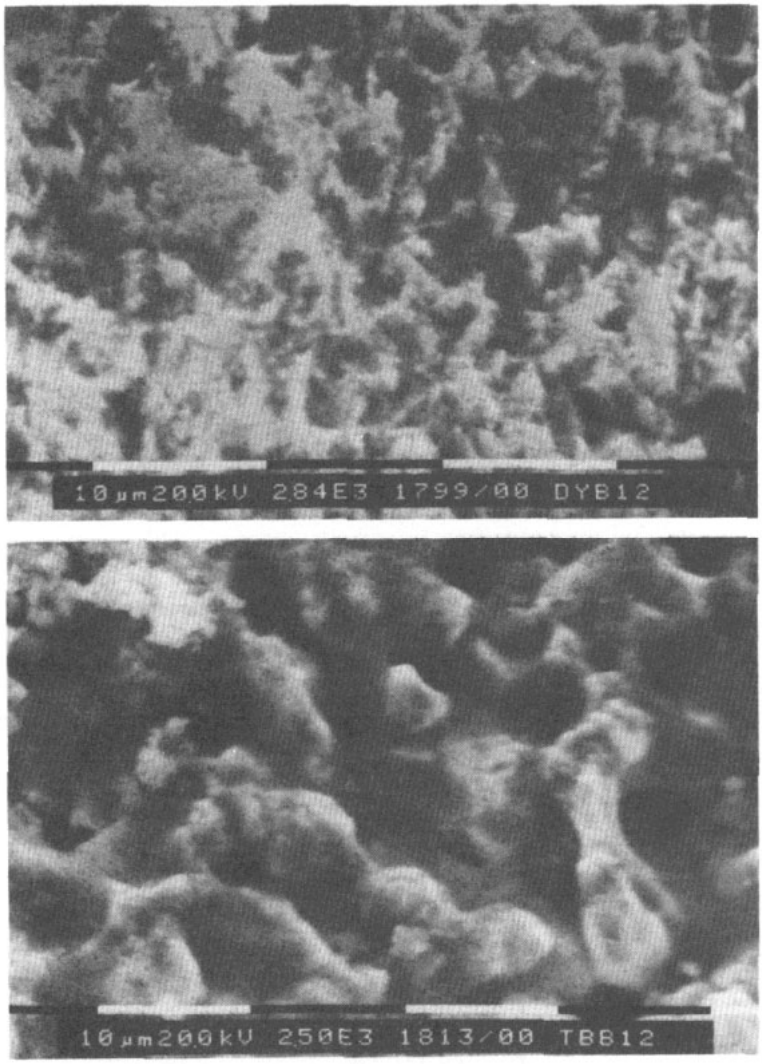

Figure 2. SEM photographs of the surface of a (upper panel) polycrystalline sample of DyB_{12} and a (lower panel) sintered sample of TbB_{12}.

The electronic thermal conductivity may be described by the following formula [15]:

$$\lambda_e = \left(\frac{\beta}{T} + \alpha T^2\right)^{-1}. \tag{4}$$

The first term is responsible for the electron scattering on impurities and physical defects whereas the second is responsible for the electron scattering on phonons. Electrons are also scattered on magnons in the temperature range below T_N and on the disordered spins of the 4f electrons above T_N [16]. Below T_N, there is no theoretical formula describing the electron–magnon scattering. Above T_N, the thermal resistivity resulting from electron scattering on the disordered spins is inversely proportional to temperature.

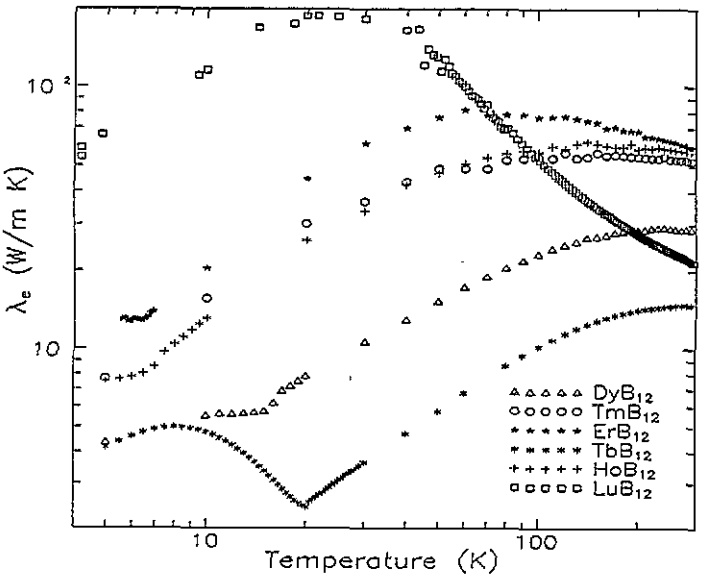

Figure 3. Temperature dependence of the electronic thermal conductivity λ_e.

The temperature dependence of the electronic thermal conductivity of our samples in the region of the paramagnetic-to-antiferromagnetic transition may be described as follows:

$$\lambda_e(TbB_{12}) = \begin{cases} 87.505T^{-1.207} & \text{below } T_N(16.9\text{–}19.2\text{ K}) \\ 0.146T^{0.944} & \text{above } T_N(19.2\text{–}30\text{ K}) \end{cases}$$

$$\lambda_e(ErB_{12}) = \begin{cases} 14.304T^{-0.058} & \text{below } T_N(5.0\text{–}6.4\text{ K}) \\ 2.974T^{0.786} & \text{above } T_N(6.4\text{–}6.7\text{ K}) \\ 1.820T^{1.049} & \text{above } T_N(6.4\text{–}10.0\text{ K}) \end{cases}$$

$$\lambda_e(DyB_{12}) = \begin{cases} 4.824T^{0.064} & \text{below } T_N(11.0\text{–}15.0\text{ K}) \\ 0.042T^{1.805} & \text{above } T_N(16.0\text{–}17.0\text{ K}) \\ 0.787T^{0.768} & \text{above } T_N(17.0\text{–}30.0\text{ K}) \end{cases}$$

$$\lambda_e(HoB_{12}) = \begin{cases} 5.144T^{0.234} & \text{below } T_N(5.0\text{–}6.5\text{ K}) \\ 0.247T^{1.820} & \text{above } T_N(7.0\text{–}7.5\text{ K}) \\ 1.148T^{1.059} & \text{above } T_N(7.5\text{–}10.0\text{ K}). \end{cases}$$

A precise description of the electronic thermal conductivity is possible only for the TbB_{12} sample, both below and above the magnetic transition. For the remaining REB_{12} compounds examined, at least two power functions of $\lambda_e(T)$ may be fitted for temperatures above T_N. Fluctuation effects may be present for both spin–electron and electron–phonon interactions [17]. They should be observable, among other things, in a variation in the electronic thermal conductivity. Much below T_N, electron–magnon interactions may be of a small-angle inelastic nature, with emission or absorption of magnons which, as bosons, are independently created and destroyed. The above mechanisms (impurity and defect scattering; first term in equation (4)) are responsible both for the weak temperature dependence of the electronic contribution for ErB_{12}, HoB_{12} and DyB_{12}, and for the maximum in the $\lambda_e(T)$ for TbB_{12}

in the temperature range 8–9 K. The abrupt change in the electronic thermal conductivity of TbB_{12} at $T_N = 19.2$ K confirms the predomiinant inelastic electron–magnon scattering within the 10.0–19.2 K range.

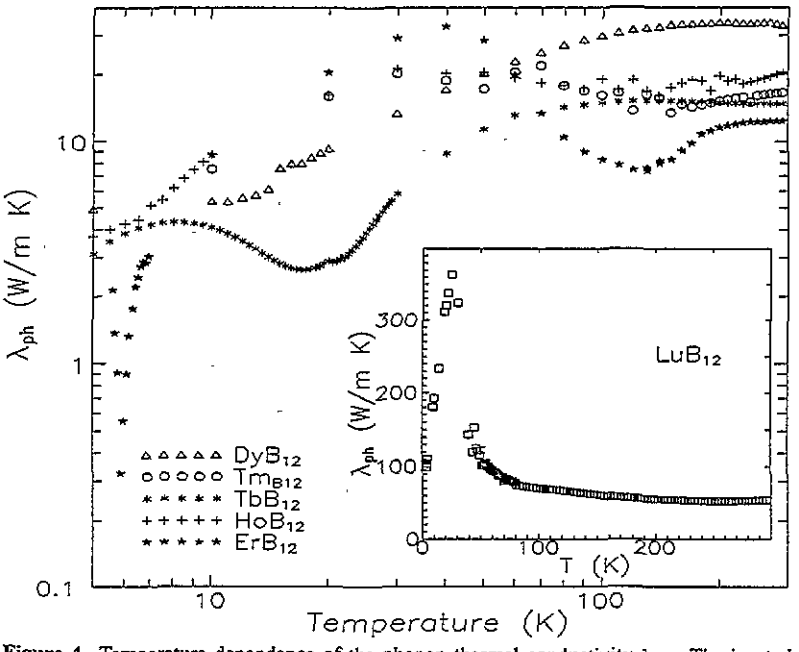

Figure 4. Temperature dependence of the phonon thermal conductivity λ_{ph}. The inset shows λ_{ph} for LuB_{12}.

Figure 4 shows the phonon thermal conductivity based on the formula

$$\lambda_{ph} = \lambda - \lambda_e. \tag{5}$$

Below the Debye temperature Θ_D, phonons are scattered by electrons ($\lambda_{ph,e} \propto T^2$), grain boundaries ($\lambda_{ph,g} \propto T^3$), point defects ($\lambda_{ph,pd} \propto T^{-1}$), dislocations ($\lambda_{ph,d} \propto T^2$) and magnons ($\lambda_{ph,m} \propto T^?$). At temperatures $T \geqslant T_{max}$ (T_{max} corresponds to the maximum value of λ), the decisive role in the phonon heat transport is played by the umklapp processes, responsible for temperature dependences of $\lambda_{ph,ph} \propto \exp[\Theta_D/T]$ type close to Θ_D and $\lambda_{ph,ph} \propto T^{-1}$ at higher temperatures.

Among the REB_{12} compounds examined, only in LuB_{12} does the phonon thermal conductivity resemble that characteristic for dielectrics (pronounced maximum at about 25 K and $\lambda_{ph} \propto 1/T$ dependence at higher temperatures (figure 4)). In magnetic REB_{12} compounds there are discrepancies between experimental results and theoretical predictions, both above and below T_N. Therefore, we confine ourselves to a presentation of the temperature dependences of the phonon thermal conductivity in the vicinity of the magnetic transition:

$$\lambda_{ph}(TbB_{12}) = \begin{cases} 0.248T^{0.820} & \text{below } T_N \text{(18.0–20.0 K)} \\ 0.232T^{0.831} & \text{above } T_N \text{(20.5–22.0 K)} \\ 0.0067T^{1.973} & \text{above } T_N \text{(22.0–22.5 K)} \end{cases}$$

$$\lambda_{ph}(ErB_{12}) = \begin{cases} 2.565 \times 10^{26}T^{-34.788} & \text{below } T_N \text{(5.6–5.9 K)} \\ 7.632 \times 10^{-23}T^{28.082} & \text{above } T_N \text{(5.9–6.2 K)} \end{cases}$$

$$\lambda_{ph}(DyB_{12}) = \begin{cases} 1.501T^{0.528} & \text{below } T_N(11.0\text{–}14.0\ \text{K}) \\ 1.064T^{0.720} & \text{above } T_N(15.0\text{–}20\ \text{K}) \\ 0.628T^{0.898} & \text{above } T_N(17.0\text{–}40.0\ \text{K}) \end{cases}$$

$$\lambda_{ph}(HoB_{12}) = \begin{cases} 1.274T^{0.670} & \text{below } T_N(5.0\text{–}6.5\ \text{K}) \\ 0.194T^{1.660} & \text{above } T_N(7.5\text{–}9.5\ \text{K}) \\ 0.151T^{1.780} & \text{above } T_N(7.5\text{–}8.5\ \text{K}). \end{cases}$$

Noticeably, the dependence of λ_{ph} versus T around T_N for TbB_{12} is almost linear, whereas there is a distinct variation for ErB_{12}. A minimum of $\lambda_{ph}(T)$ is seen for ErB_{12} at around 120 K. At temperatures close to 100 K, the phonon scattering by paramagnetic levels split by the crystal field is considerable [16]. Above T_N, as for electronic thermal conductivity, the phonon contribution may be described by at least two power functions.

For ferromagnets, below the Curie temperature T_C, the theory predicts $\lambda_m \propto T^2$ [18] whereas, for antiferromagnets, below T_N, $\lambda_m(T) \propto T^3$ [19]. The above-presented method of calculation of $\lambda_{ph}(T)$ assumes that there is a magnon contribution to the heat transport below the transition temperature. Besides magnons, a substantial influence on $\lambda(T)$ is exerted by the crystal electric field (CEF) effects, the aspherical shape of the 4f shell and the presence of magnetic impurities.

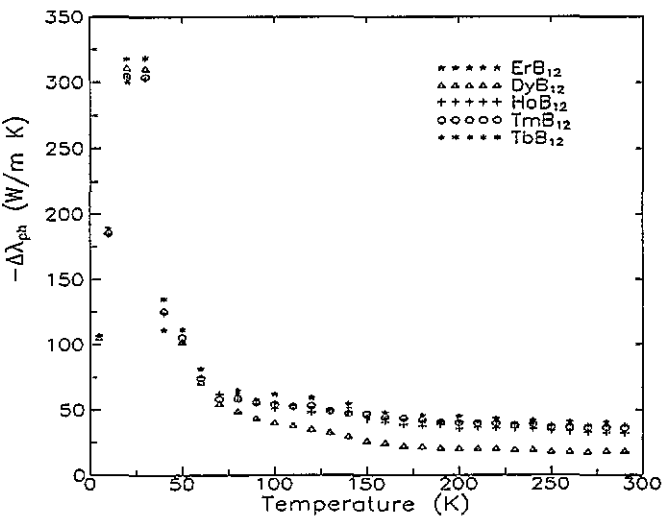

Figure 5. Temperature dependence of $-\Delta\lambda_{ph}$ for the analysed samples.

The magnetic contribution to the phonon and electronic thermal conductivities (figures 5 and 6) was calculated from the formulae

$$\Delta\lambda_{ph}(T) = \lambda_{ph}(REB_{12}) - \lambda_{ph}(LuB_{12}) \tag{6}$$

$$\Delta\lambda_e(T) = \lambda_e(REB_{12}) - \lambda_e(LuB_{12}). \tag{7}$$

In the REB_{12} compounds, two types of phonon spectrum may be distinguished [20]: a high-temperature spectrum, associated with vibrations of the B-atom sublattice, and a low-temperature spectrum, connected with RE atom vibrations. Below 65 K, all the samples display similar behaviours, with an almost linear temperature dependence below $T_{max} = 30$ K (see figure 5). Above 65 K, except for DyB_{12}, all the samples exhibit a

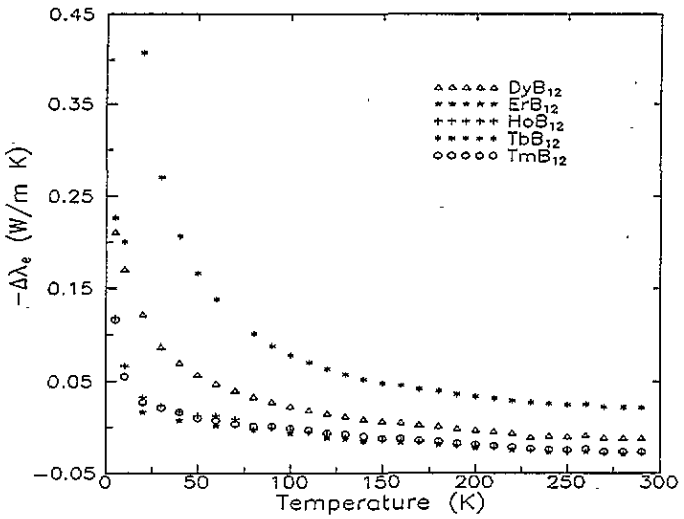

Figure 6. Temperature dependence of $-\Delta\lambda_e$ for REB_{12} samples.

$-\Delta\lambda_{ph} \propto 1/T$ dependence. The latter results in the predominant role of the phonon–phonon interactions at high temperatures for TbB_{12}, HoB_{12}, ErB_{12} and TmB_{12}. For DyB_{12}, phonon heat transport at higher temperatures is governed by phonon–phonon and phonon–paramagnetic impurity scattering. It should be stressed that equations (6) and (7) do not consider the processes of scattering of phonons and electrons on physical defects. Each of the samples investigated should, in our opinion, exhibit the same amount of these defects. If the ratio $\rho_{300\ K}/\rho_{4.2\ K}$ of the electrical resistivity at room temperature to that at liquid-helium temperature, is adopted as the measure of the physical defect rate, our samples show some scatter in this quantity, as seen in table 2.

Table 2. Resistance ratio $\mathcal{R} \equiv \rho_{300\ K}/\rho_{4.2\ K}$ for dodecaborides analysed.

Sample	$\mathcal{R}$
LuB_{12}	71.93
TbB_{12}	15.30
DyB_{12}	9.54
HoB_{12}	13.50
ErB_{12}	17.46
TmB_{12}	8.89

The temperature dependence of $-\Delta\lambda_e(T)$ presented in figure 6 reveals a large difference between the magnitudes of the electronic thermal conductivity at low temperatures for TbB_{12} and DyB_{12}, the difference decreasing with temperature increase.

In the paramagnetic region the electrical resistivity is inversely proportional to the thermal conductivity. It may be presented as

$$\rho(T) = \rho_0 + \rho_{ph} + \rho_m \tag{8}$$

where ρ_0, ρ_{ph} and ρ_m are the residual, phonon and magnetic terms, respectively, with

$$\rho_m = \rho_{spd} \propto \text{constant}(g-1)^2\mathcal{J}(\mathcal{J}+1) \tag{9}$$

where ρ_{spd} denotes the electrical resistivity due to the spin-disorder scattering, g is the Landé factor and $\mathcal{J}$ is the total angular momentum.

According to theory [21], $-\Delta\lambda_e$ is proportional to T above the transition point, provided that the influence of the CEF effect is negligible. The formula $-\Delta\lambda_e(T)$ was obtained assuming W–F law validity, which is equivalent to another assumption that there is only small-angle elastic electron–phonon scattering. The results presented in figure 6 show that the $-\Delta\lambda_e \propto T$ dependence is not obeyed above T_N, which in turn may suggest a substantial CEF effect on electronic heat transport. The presence of the large-angle inelastic electron–phonon interactions may be taken into account as well. To estimate the qualitative contribution of the CEF effects to electronic heat transport in REB_{12}, the temperature dependence of L_{CF}/L_0 was shown in figure 7. L_{CF} was calculated from the formula

$$L_{CF} = (\Delta\rho\Delta\lambda_e)/T \tag{10}$$

where $\Delta\rho = \rho(REB_{12}) - \rho(LuB_{12})$ and $\Delta\lambda_e$ is as in equation (7).

As shown in figure 7, apart from some temperature regions, L_{CF}/L_0 is close to unity. For TmB_{12}, a sharp increase in L_{CF}/L_0 up to +2.8 at 75 K and a sharp decrease down to −2.7 for HoB_{12} is observed at 90 K.

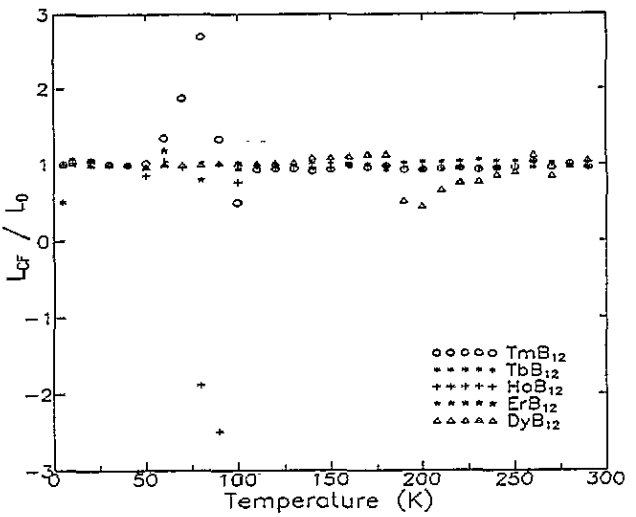

Figure 7. Temperature dependence of the ratio L_{CF}/L_0.

The invalidity of the W–F law in this case may result from

(a) the different intensities of the electron–phonon scattering for thermal and electrical conductivities,

(b) the complex f-band-structure energy dependence of the relaxation time and

(c) an increase in the interband transition number.

4. Conclusions

Experimental study of the compounds with REB_{12} stoichiometry shows that they constitute an interesting system for studying the effect of 4f electrons on heat transport.

In particular, we found the following.

(1) Over a magnetically ordered range, the contribution of magnons to heat transport is observable.

(2) The electronic and phonon thermal conductivities exhibit distinct difference at the Néel temperature.

(3) The rest in λ_{ph} at the transition to the antiferromagnetic phase can be attributed to the magnon component λ_m.

(4) The value L_{CF}/L_0 equals approximately 1 in the whole temperature range, except for TmB_{12} and HoB_{12} which show anomalies at temperatures of around 75 K and 90 K, respectively. This may evidence a complex band structure of these compounds.

(5) The influence of the CEF on the electronic component of thermal conductivity was observed at $T > T_N$.

(6) The phonon–phonon interaction determines the heat transport by phonons at $T \gg T_N$.

(7) We suppose that in REB_{12} the 4f electrons with spin fluctuations are playing an important role in the heat transport.

The influence that the 4f electrons exert on the thermal conductivity will be subject to further investigation.

Acknowledgment

This work was partly supported by the Polish State Committee for Scientific Research under grant 8S501 057 04.

References

[1] Spear K E 1977 *Boron and Refractory Borides* ed V I Matkovich (Berlin: Springer) pp 439–56
[2] Cannon J F, Cannon D M and Hall H T 1979 *High-Pressure Science and Technology* vol 1, ed K I Timmerhaus and M S Barber (New York: Plenum) p 100
[3] Matkovich V I, Economy J, Giese R F and Barret R 1965 *Acta Crystallogr.* **19** 1056
[4] Kasaya M, Iga F, Takigawa M and Kasuya T 1985 *J. Magn. Magn. Mater.* **47–48** 429
[5] Kasaya M, Iga F, Negishi K, Nakai S and Kasuya T 1983 *J. Magn. Magn. Mater.* **31–34** 437
[6] Sugiyama K, Iga F, Kasaya M, Kasaya T and Data M 1988 *J. Phys. Soc. Japan* **57** 3946
[7] Touloukian Y S, Powell R W, Ho C Y and Klemens P G 1979 *Thermal Conductivity, Metallic Elements and Alloys* (Washington: IFI–Plenum)
[8] Moiseenko L L and Odintsov V V 1979 *J. Less-Common Met.* **67** 237
[9] Moiseenko L L and Paderno Y 1982 *Izv. Vyssh. Uchebn. Zaved. Fiz.* **25** 119
[10] Matthias B T, Geballe T H, Andres K, Corenzwit E, Hull G W and Maita J P 1968 *Science* **159** 530
[11] Odintsov V V, Lesnaya M I and Lvov S N 1973 *At. Energy* **35** 134
[12] Paderno Y, Filippov V and Shitsevalova N 1991 *Boron-Rich Solids 1990 (AIP Conf. Proc. 231)* (New York: American Institute of Physics) p 460
[13] Jeżowski A, Mucha J and Pompe G 1987 *J. Phys. D: Appl. Phys.* **20** 1500
[14] Paderno Y, Filippov V, Shitsevalova N, Batko I and Flahbart K 1994 *Japan. J. Appl. Phys. Suppl.* **10** 154
[15] Wilson A H 1953 *The Theory of Metals* (Cambridge: Cambridge University Press)
[16] Rives J E and Walton D 1968 *Phys. Lett.* **27** 609
[17] Smirnov I A and Oskotski V S 1993 *Thermal Conductivity of Rare Earth Compounds (Handb. Phys. Chem. Rare Earths 16)* ed K A Gschneidner (Amsterdam: Elsevier)
[18] Yelon W B and Berger L 1970 *Phys. Rev. Lett.* **25** 17
[19] Klemens P G 1969 *Thermal Conductivity* vol 1, ed R P Tye (London: Academic)
[20] Hamada K, Wakuta M, Sugii N, Matsuura K, Kubo K and Yamauchi H 1993 *Phys. Rev.* B **48** 10
[21] Bauer E, Gratz E and Adam G 1986 *J. Phys. F: Met. Phys.* **16** 493